

Btk activation of sustained Ca²⁺ mobilization in response to secretory immunoglobulin M (19). Thus, Rlk, a distinct Tec kinase that functions independently of PI3K, may provide a second level of regulation to antigen receptor signaling pathways in T cells.

Current models suggest that immune responses in lymphocytes are exquisitely controlled, requiring multiple finely tuned levels of activation (20). Thus, the Tec kinases, unlike the more proximally acting Lck and Zap-70, may not serve as primary triggers of the immune response but instead may further refine the strength of lymphocyte signaling by acting as critical modulators of PLC-γ and downstream effectors.

References and Notes

1. A. Weiss and D. R. Littman, *Cell* **76**, 263 (1994); R. L. Wange and L. E. Samelson, *Immunity* **5**, 197 (1996).
2. D. B. Straus and A. Weiss, *Cell* **70**, 585 (1992); B. L. Williams *et al.*, *Mol. Cell. Biol.* **18**, 1388 (1998).
3. S. Desiderio and J. D. Siliciano, *Chem. Immunol.* **59**, 191 (1994).
4. D. J. Rawlings and O. N. Witte, *Semin. Immunol.* **7**, 237 (1995).
5. M. F. Bachmann, D. R. Littman, X. C. Liao, *J. Virol.* **71**, 7253 (1997).
6. R. N. Haire *et al.*, *Hum. Mol. Genet.* **3**, 897 (1994); Q. Hu *et al.*, *J. Biol. Chem.* **270**, 1928 (1995); C. L. Sommers *et al.*, *Oncogene* **11**, 245 (1995).
7. J. Debnath *et al.*, *Mol. Cell. Biol.* **19**, 1498 (1999).
8. E. Schaeffer, J. Debnath, P. Schwartzberg, unpublished results.
9. X. C. Liao and D. R. Littman, *Immunity* **3**, 757 (1995).
10. The near normal mature T cell numbers in *rlk*^{-/-}*itk*^{-/-} mice may result from differential requirements for Itk and Rlk during T cell development versus mature T cell activation or compensatory expression of Tec in thymocytes. However, preliminary evidence from TCR transgenic mice suggests that combined deficiency of Rlk and Itk decreases selection processes with a switch from negative to positive selection that may account for increased cellularity in *rlk*^{-/-}*itk*^{-/-} mice relative to *itk*^{-/-} mice (8).
11. K. Q. Liu, S. C. Bunnell, C. B. Gurniak, L. J. Berg, *J. Exp. Med.* **187**, 1721 (1998).
12. M. J. Lenardo, *Semin. Immunol.* **9**, 1 (1997).
13. D. Y. Noh, S. H. Shin, S. G. Rhee, *Biochim. Biophys. Acta* **1242**, 99 (1995).
14. O. Sozeri *et al.*, *Oncogene* **7**, 2259 (1992); W. Kolch *et al.*, *Nature* **364**, 249 (1993).
15. Graded biochemical defects were observed in mutant cells, with *rlk*^{-/-} appearing similar to wild-type cells and *itk*^{-/-} more closely resembling the *rlk*^{-/-}*itk*^{-/-} phenotype.
16. MAP kinase activation in T lymphocytes also occurs through GRB-2-mediated pathways (21). However, tyrosine-phosphorylated proteins bound by GRB-2's SH2 domain, including Cbl, Slp-76, and LAT (21, 22), were normal in mutant cells (8), suggesting intact GRB-2-mediated signals.
17. T. M. Scharton-Kersten and A. Sher, *Curr. Opin. Immunol.* **9**, 44 (1997); E. Y. Denkers *et al.*, in *Host Response to Intracellular Pathogens*, S. H. E. Kaufman, Ed. (Landes, Austin, TX, 1997), pp. 167-181.
18. D. Yablonski, M. R. Kuhne, T. Kadlecck, A. Weiss, *Science* **281**, 413 (1998).
19. A. M. Scharenberg and J. P. Kinet, *Cell* **94**, 5 (1998).
20. J. Sloan-Lancaster and P. M. Allen, *Annu. Rev. Immunol.* **14**, 1 (1996); J. Madrenas and R. N. Germain, *Semin. Immunol.* **8**, 83 (1996).
21. D. Cantrell, *Annu. Rev. Immunol.* **14**, 259 (1996).
22. W. Zhang, J. Sloan-Lancaster, J. Kitchen, R. P. Triple, L. E. Samelson, *Cell* **92**, 83 (1998).
23. Purified splenocytes (5 × 10⁶) were stimulated for indicated times with plate-bound 2C11 (7.5 μg/ml), lysed in 1% Triton and 0.1% SDS in phosphate-buffered saline with protease inhibitors (Boehringer

Mannheim) and sodium vanadate, and immunoprecipitated with either anti-TCR zeta chain (gift of L. Samelson) or anti-Zap-70 (Upstate). Immune complexes were resolved by 10% SDS-polyacrylamide gel electrophoresis (SDS-PAGE) and immunoblotted with anti-phosphotyrosine (4G10 Upstate).

24. pMC1neo and multiple stop codons were inserted into the Kpn I site of *rlk* (encoding the start of the SH2 domain) with 6-kb upstream and 3-kb downstream sequences, followed by herpes simplex virus thymidine kinase (HSV-TK). The construct was electroporated into TC1 ES cells and G418-gancyclovir-resistant colonies screened by Southern (DNA) blot analyses with Hind III and a flanking 3' probe. Gene disruption at the 5' end was confirmed with an internal probe.
25. Splenocytes were stimulated with PMA (10 ng/ml) and ionomycin (1 μg/ml) for 24 hours to ensure equal proliferation, washed, and grown with IL-2 for 3 days. Cells were restimulated with anti-CD3ε (2C11) for 24 hours, and cell viability was determined by flow cytometry.
26. Internal Ca²⁺ in purified T cells (5 × 10⁶ per millili-

ter) loaded with Fluo-3-AM (5 μg/ml) and Fura-Red-AM (5 μg/ml) (Molecular Probes, Eugene, OR) (13) was analyzed with MultiTime Kinetic Experiment Analysis Software (Phoenix Flow Systems, San Diego, CA), and data were expressed as percentage responding relative to unstimulated cells.

27. Purified splenic T cells (4.0 × 10⁷) were stimulated (23) and examined by IP₃ Radioreceptor Assay Kit (NEN Life Science).
28. E. Y. Denkers *et al.*, *J. Immunol.* **159**, 1903 (1997).
29. We thank L. Samelson, J. O'Shea, J. Dodson, and R. Nussbaum for comments; A. Wynshaw-Boris, C. Canina, and D. Bernards for assistance with ES cells; S. Anderson for flow cytometry; and M. Czar, A. Venegas, W. Hively, C. Elliot, M. Chamorro, L. Brody, E. Arnold, M. Erdos, L. Zheng, B. Combediere, and R. Siegel. Animal care was in accordance with NIH guidelines. This work was initiated in the laboratory of M.J.L., continued in the laboratory of H.E.V., and completed in the laboratory of P.L.S. E.M.S. and J.D. are Howard Hughes Medical Institute-NIH Research Scholars.

18 December 1998; accepted 15 March 1999

Efficient Persistence of Extrachromosomal KSHV DNA Mediated by Latency-Associated Nuclear Antigen

Mary E. Ballestas,¹ Pamela A. Chatis,^{2,3} Kenneth M. Kaye^{1*}

Primary effusion lymphoma (PEL) cells harbor Kaposi's sarcoma-associated herpesvirus (KSHV) episomes and express a KSHV-encoded latency-associated nuclear antigen (LANA). In PEL cells, LANA and KSHV DNA colocalized in dots in interphase nuclei and along mitotic chromosomes. In the absence of KSHV DNA, LANA was diffusely distributed in the nucleus or on mitotic chromosomes. In lymphoblasts, LANA was necessary and sufficient for the persistence of episomes containing a specific KSHV DNA fragment. Furthermore, LANA colocalized with the artificial KSHV DNA episomes in nuclei and along mitotic chromosomes. These results support a model in which LANA tethers KSHV DNA to chromosomes during mitosis to enable the efficient segregation of KSHV episomes to progeny cells.

Kaposi's sarcoma (KS)-associated herpesvirus or human herpesvirus-8 likely plays an important role in KS pathogenesis because KSHV seropositivity precedes KS and KSHV DNA is found in almost all KS lesions, whether or not there is a coexisting human immunodeficiency virus infection (1). KSHV is also associated with lymphoproliferative disorders, including PELs and multicentric Castlemann's disease (2, 3).

Similar to the gamma-1 herpesvirus Epstein-Barr virus (EBV), KSHV infection in tu-

mor tissue or in lymphoma-derived cell lines is predominantly latent. Latently infected cells have multiple copies of circularized KSHV DNA maintained as episomes (2-4). The EBV nuclear antigen-1 (EBNA1) protein mediates efficient episome persistence through a cis-acting 1.8-kb EBV DNA sequence, which is termed the origin of plasmid replication (oriP) (5, 6). Herpesvirus saimiri (HVS) also has a cis-acting sequence that enables the efficient persistence of episomes in HVS-infected cells (7). However, KSHV has no obvious homology to the EBV or HVS cis-acting DNA, and a trans-acting EBNA1 homolog or analog has not been identified in HVS or in other gamma-2 herpesviruses.

KSHV open reading frame (ORF) 73 encodes the latency-associated nuclear antigen (LANA, LNA, or LNA1), which is predicted to be 1162 amino acids, and lacks a known function (1, 8, 9). A homologous ORF exists in other gamma-2 herpesviruses (10). LANA is

¹Department of Medicine, Channing Laboratory, Brigham and Women's Hospital, Harvard Medical School, 181 Longwood Avenue, Boston, MA 02115, USA. ²Department of Medicine, Beth Israel Deaconess Medical Center, Harvard Medical School, 330 Brookline Avenue, Boston, MA 02215, USA. ³NEN Life Science Products, 549 Albany Street, Boston, MA 02118, USA.

*To whom correspondence should be addressed. E-mail: kkaye@rics.bwh.harvard.edu

REPORTS

reactive with most KSHV-immune sera that detect LANA in KSHV-infected PEL cells and in KS spindle cells (9, 11, 12).

The previously described punctate distribution (9, 11, 12) of LANA in PEL cells was further investigated by confocal microscopy. LANA was detected with immune serum, and KSHV DNA was detected by fluorescence in situ hybridization (FISH) in KSHV-infected BCBL-1 PEL cells (11, 13). Two-color confocal microscopy demonstrated that LANA (Fig. 1A, green signal) and KSHV DNA (Fig. 1B, red signal) colocalized (Fig. 1C, yellow signal) in subnuclear dots that were multiple, small, and discrete. Each dot probably corresponds to a KSHV DNA episome because ~40 dots were visualized in each nucleus, which is consistent with estimates of the KSHV genome copy number per cell (2, 3). LANA was highly concentrated at sites of KSHV DNA. The finding that LANA is restricted to sites of KSHV DNA in interphase was previously unknown and is indicative of specific recognition of KSHV DNA by LANA.

We next investigated whether the association of LANA and KSHV DNA persisted in mitosis. LANA (12) and KSHV DNA (2) associate with mitotic chromosomes in PEL cells. Colocalization of LANA and KSHV DNA on chromosomes would be consistent with a role for LANA in episome persistence. Therefore, we detected KSHV DNA in BCBL-1 cells with

FISH (Fig. 2A, red signal), we detected LANA with immune serum (Fig. 2B, green signal), and we detected chromosomes with 4',6'-diamidino-2-phenylindole (DAPI) (Fig. 2C, blue signal) (13). An overlay of the same chromosome spread (Fig. 2, A through C) revealed LANA to be highly localized to sites of KSHV DNA, and both LANA and KSHV DNA were in dots dispersed widely over the metaphase chromosomes without apparent regularity (Fig. 2D, punctate white on blue chromosomes). The finding that LANA colocalizes with KSHV genomes on metaphase chromosomes is consistent with a model in which LANA mediates the segregation of KSHV episomes to progeny cells by linking KSHV DNA to chromosomes during mitosis.

If this model were correct, LANA, independent of other KSHV proteins, would mediate KSHV episome persistence in proliferating cells. To directly test this hypothesis, we stably expressed LANA or a FLAG-tagged LANA (F-LANA) in KSHV- and EBV-negative BJAB B lymphoma cells (14). Because the HVS oriP is located near the start of the viral genome (7) and because the KSHV genome is generally colinear with that of HVS, we considered the possibility that the KSHV oriP is in a cosmid clone (Z6) (8) that contains the terminal repeats and the start of the KSHV genome. Z6 or a

cosmid (Z8) (8) that contains sequence from near the center of the KSHV genome was transfected into BJAB cells or into LANA- or F-LANA-expressing BJAB cells (BJAB/LANA or BJAB/F-LANA, respectively). Cells were selected for G418 resistance conferred by the cosmid vector (14). Z6 cosmid DNA efficiently persisted in BJAB/LANA and BJAB/F-LANA cells, and almost all (99%) microtiter wells were positive for G418-resistant cell outgrowth. Efficient persistence of Z6 DNA was dependent on LANA because only 7% of the wells of LANA-negative BJAB cells transfected with Z6 were positive for outgrowth. In contrast to Z6, Z8 lacked a cis-acting component necessary for efficient LANA-mediated outgrowth, and only 3% of wells containing Z8-transfected BJAB/F-LANA cells were positive for G418-resistant outgrowth. The same low level of persistence was observed in Z8-transfected BJAB cells that were LANA negative. These results are reminiscent of those obtained with EBV oriP and EBNA1, in which EBNA1 enabled a 10- to 100-fold increase of outgrowth for cells transfected with oriP DNA, in comparison with non-oriP DNA (5).

The distribution of F-LANA in BJAB cells was investigated with immunofluorescent microscopy after detection with immune serum or monoclonal antibody to FLAG (15). F-LANA was distributed diffusely in interphase nuclei (Fig. 3A) and on chromosomes (Fig. 3C) in BJAB/F-LANA cells, but F-LANA was focally concentrated to dots in interphase nuclei (Fig. 3B) and along chromosomes (Fig. 3D) in BJAB/F-LANA cells that were Z6 transfected and G418 resistant. Simultaneous detection of F-LANA and Z6

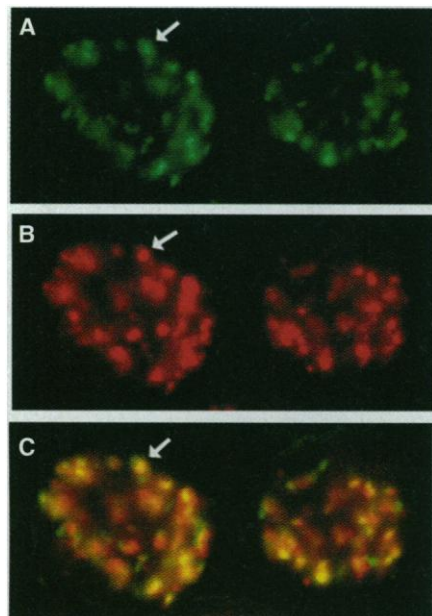


Fig. 1. LANA colocalizes with KSHV episomes. (A) LANA was detected with KSHV immune serum (green signal), and (B) KSHV episomes were detected with FISH (red signal) in the same BCBL-1 cells. (C) Overlay of (A) and (B) results in a yellow signal at sites of colocalization. The arrows indicate one site of colocalization. Confocal microscopy was performed with a Zeiss Axioskop, PCM2000 hardware, and C-imaging software (magnification, $\times 630$).

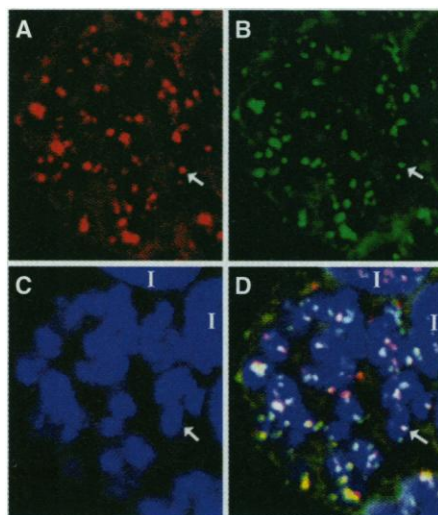


Fig. 2. LANA associates with KSHV genomes on chromosomes. BCBL-1 cells were metaphase arrested with colcemid and swollen in hypotonic buffer. (A) KSHV genomes were detected with FISH (red signal), (B) LANA was detected with KSHV-immune serum (green signal), and (C) chromosomes were detected with DAPI (blue signal) (13). The same mitotic cell is shown in (A), (B), and (C). (D) Overlay of panels (A), (B), and (C). A white signal results when a KSHV genome and LANA colocalize on a chromosome. The arrows indicate one site of colocalization. "I" indicates adjacent interphase nuclei. Staining was detected with a Zeiss Axiovert S100 microscope fitted with Biorad MRC1024/2P confocal hardware, a Multiphoton Tsunami Laser, and Biorad Lasersharp 3.1 software (magnification, $\times 630$).

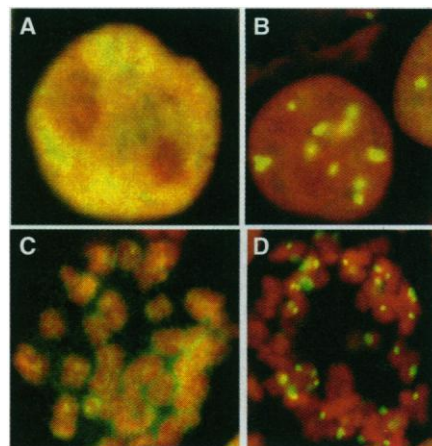


Fig. 3. LANA concentrates to dots with Z6 KSHV DNA. (A and C) BJAB/F-LANA cells and (B and D) BJAB/F-LANA cells transfected with Z6 were stained with propidium iodide (red signal) to detect interphase nuclei (A and B) or metaphase chromosomes (C and D) and KSHV immune serum (green signal) to visualize LANA. Colocalization of nucleic acid and LANA results in yellow signal. Confocal microscopy was performed as in Fig. 1 (magnification, $\times 630$).

REPORTS

DNA demonstrated that F-LANA concentrated to dots at sites of Z6 DNA (15). In contrast to Z6-transfected cells, F-LANA remained diffusely distributed in the nuclei of BJAB/F-LANA cells that were Z8 transfected and G418 resistant (15). These data demonstrate that LANA specifically localizes to sites of Z6 KSHV DNA, which is consistent with the hypothesis that LANA serves to tether Z6 DNA to chromosomes.

If LANA mediates the efficient segregation of KSHV episomes to progeny cells, then LANA-expressing cells that are Z6 transfected and G418 resistant should contain extrachromosomal Z6 DNA. Extrachromosomal DNA should rarely or never be found in G418-resistant cells that are Z6 transfected and LANA negative or Z8 transfected and LANA positive. Gardella gel analysis followed by Southern (DNA) blotting was performed to determine whether Z6 DNA is an episome in BJAB/LANA and BJAB/F-LANA cells. In Gardella gels, live cells are lysed in situ in the gel-loading wells at the start of the gel run. Episomal DNA (as large as 200 kb) migrates into the gel, whereas chromosomal DNA is unable to migrate into the gel (16). As expected, BCBL-1- [Fig. 4, A (lane 1) and B (lane 4)] and KSHV-infected BC-1 PEL cells (2) (Fig. 4B, lane 2) had episomal KSHV DNA, whereas KSHV-negative Raji [Fig. 4, A (lane 2) and B (lane 1)] and BJAB (Fig. 4B,

lane 3) cells lacked KSHV episomes. BJAB/LANA cells (Fig. 4A, lanes 3 through 7) or BJAB/F-LANA cells (Fig. 4A, lanes 8 through 12) that had grown out after transfection with Z6 DNA and G418 selection also had extrachromosomal DNA. In contrast, BJAB/F-LANA cells that had grown out after transfection with Z8 DNA and G418 selection did not have extrachromosomal Z8 DNA (Fig. 4B, lanes 5 through 12). Also, LANA-negative BJAB cells that had grown out as G418 resistant after transfection with Z6 or Z8 did not have episomal DNA (15). These latter cells had Z6 or Z8 DNA, as determined by polymerase chain reaction, and Z6 or Z8 DNA was sometimes detected at the loading wells on long exposures of Southern blots of Gardella gels, which is consistent with the presence of integrated DNA in these cells. These experiments demonstrate that LANA acts in-trans on a cis-acting element present in Z6 to efficiently mediate Z6 episome persistence in cells.

To more precisely localize the Z6 cis-acting element, Hind III subclones of Z6 cosmid DNA were transfected into BJAB or BJAB/F-LANA cells and selected for G418 resistance (14). A Z6 subclone containing the terminal repeats and the first ~13 kb of the KSHV genome (Z6-13) efficiently persisted as an episome in G418-resistant BJAB/F-LANA cells (Fig. 4C, lanes 6

through 9). In contrast, BJAB/F-LANA cells that had grown out as G418 resistant after transfection of Hind III subclones containing ~7 or ~11 kb of downstream KSHV sequence (Z6-7 and Z6-11, respectively) did not have extrachromosomal Z6-7 (Fig. 4C, lanes 12 and 13) or Z6-11 DNA (15). LANA-negative BJAB cells that had grown out as G418 resistant after transfection with Z6-13 (Fig. 4C, lanes 4 and 5), Z6-7 (Fig. 4C, lanes 10 and 11), or Z6-11 DNA (15) did not have episomal DNA. Therefore, LANA acts in-trans on a cis-acting element that is proximal to or in the terminal repeats of Z6 to mediate efficient episome persistence.

These results provide the first identification of a trans-acting factor that supports episome persistence of gamma-2 herpesvirus DNA. LANA acts on a cis-acting element present in a defined region of KSHV DNA to mediate the efficient persistence of episomal DNA in cells. Both EBV and HVS have dyad symmetry elements within their cis-acting plasmid maintenance sequences (5, 6, 17), and fine mapping of the cis-acting sequence in Z6 may demonstrate that a similar element is necessary for KSHV episome persistence. Because HVS and other gamma-2 herpesviruses have LANA homologs, these proteins are likely candidates to mediate episome persistence for their respective viral genomes. Whether the gamma-2 herpesvirus LANA-type proteins also share the EBNA1 property of transcriptional activation (18) remains to be evaluated.

Although LANA and EBNA1 share the property of diffuse association with chromosomes in the absence of cognate viral DNA, LANA differs from EBNA1 in highly localizing to its cognate DNA. KSHV DNA can recruit a substantial fraction of the LANA molecules in the cell. In contrast, EBNA1 is diffusely distributed on metaphase chromosomes, even in the presence of EBV DNA (6, 19, 20). LANA and EBNA1 also lack obvious sequence homology. However, EBNA1 shares structural and functional characteristics with the nonhomologous bovine papilloma virus (BPV) E2 protein (17), and LANA could have similar structural features.

The finding that LANA colocalizes with KSHV episomes on chromosomes and is sufficient for the extrachromosomal persistence of KSHV DNA supports a model in which LANA tethers KSHV episomes to chromosomes during mitosis. Complexing KSHV DNA to chromosomes would ensure an efficient distribution of episomes to progeny cells and the inclusion of KSHV DNA in newly formed nuclei. Such a model of linking episomes to chromosomes has been proposed for EBNA1 and the BPV E2 protein (5, 6, 21). Although additional work is necessary to further define the molecular mechanisms by which LANA mediates KSHV episome persistence, strategies that interfere with the functions of LANA described here could be

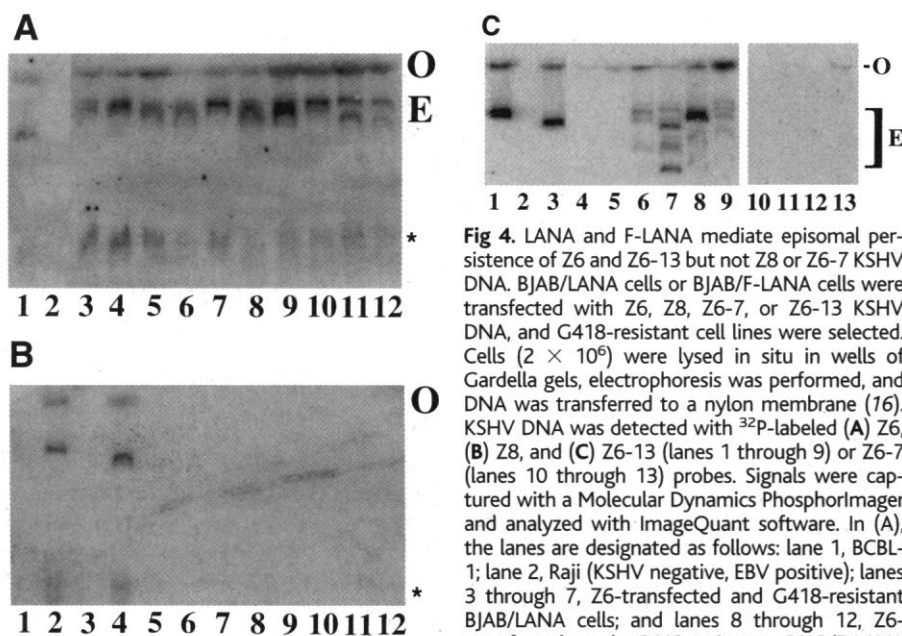


Fig 4. LANA and F-LANA mediate episomal persistence of Z6 and Z6-13 but not Z8 or Z6-7 KSHV DNA. BJAB/LANA cells or BJAB/F-LANA cells were transfected with Z6, Z8, Z6-7, or Z6-13 KSHV DNA, and G418-resistant cell lines were selected. Cells (2×10^6) were lysed in situ in wells of Gardella gels, electrophoresis was performed, and DNA was transferred to a nylon membrane (16). KSHV DNA was detected with ^{32}P -labeled (A) Z6, (B) Z8, and (C) Z6-13 (lanes 1 through 9) or Z6-7 (lanes 10 through 13) probes. Signals were captured with a Molecular Dynamics PhosphorImager and analyzed with ImageQuant software. In (A), the lanes are designated as follows: lane 1, BCBL-1; lane 2, Raji (KSHV negative, EBV positive); lanes 3 through 7, Z6-transfected and G418-resistant BJAB/LANA cells; and lanes 8 through 12, Z6-transfected and G418-resistant BJAB/F-LANA cells. The electrophoretic mobility of Z6 episomes is slower than predicted by size. In (B), lanes are designated as follows: lane 1, Raji; lane 2, BC-1; lane 3, BJAB; lane 4, BCBL-1; and lanes 5 through 12, Z8-transfected and G418-resistant BJAB/F-LANA cells. In (C), lanes are designated as follows: lane 1, BC-1; lane 2, BJAB; lane 3, BCBL-1; lanes 4 and 5, Z6-13-transfected and G418-resistant BJAB cells; lanes 6 through 9, Z6-13-transfected and G418-resistant BJAB/F-LANA cells; lanes 10 and 11, Z6-7-transfected and G418-resistant BJAB cells; and lanes 12 and 13, Z6-7-transfected and G418-resistant BJAB/F-LANA cells. Multiple episomal bands in lanes 6 through 9 (C) are likely due to duplications and deletions in the terminal repeats as demonstrated by Southern (DNA) analysis (15). The BC-1 genome differs in size from that of BCBL-1 (1, 23). O, well origins; E, episomes; *, nicked, degraded, and linear DNA.

is slower than predicted by size. In (B), lanes are designated as follows: lane 1, Raji; lane 2, BC-1; lane 3, BJAB; lane 4, BCBL-1; and lanes 5 through 12, Z8-transfected and G418-resistant BJAB/F-LANA cells. In (C), lanes are designated as follows: lane 1, BC-1; lane 2, BJAB; lane 3, BCBL-1; lanes 4 and 5, Z6-13-transfected and G418-resistant BJAB cells; lanes 6 through 9, Z6-13-transfected and G418-resistant BJAB/F-LANA cells; lanes 10 and 11, Z6-7-transfected and G418-resistant BJAB cells; and lanes 12 and 13, Z6-7-transfected and G418-resistant BJAB/F-LANA cells. Multiple episomal bands in lanes 6 through 9 (C) are likely due to duplications and deletions in the terminal repeats as demonstrated by Southern (DNA) analysis (15). The BC-1 genome differs in size from that of BCBL-1 (1, 23). O, well origins; E, episomes; *, nicked, degraded, and linear DNA.

useful in aborting latent KSHV infection and in preventing or treating KSHV-associated diseases.

Note added in proof: The Z6 cis-acting element has been further localized to three copies of the terminal repeat and up to ~600 nucleotides of unique sequence.

References and Notes

1. Y. Chang *et al.*, *Science* **266**, 1865 (1994); P. S. Moore *et al.*, *J. Virol.* **70**, 549 (1996); S.-J. Gao *et al.*, *N. Engl. J. Med.* **335**, 233 (1996); P. S. Moore and Y. Chang, *ibid.* **332**, 1181 (1995).
2. E. Cesarman *et al.*, *Blood* **86**, 2708 (1995).
3. M. B. Rettig *et al.*, *Science* **276**, 1851 (1997); J. Soulier *et al.*, *Blood* **86**, 1276 (1995); E. Cesarman, Y. Chang, P. S. Moore, J. W. Said, D. M. Knowles, *N. Engl. J. Med.* **332**, 1186 (1995).
4. L. L. Decker *et al.*, *J. Exp. Med.* **184**, 283 (1996).
5. J. Yates, N. Warren, D. Reisman, B. Sugden, *Proc. Natl. Acad. Sci. U.S.A.* **81**, 3806 (1984); J. L. Yates, N. Warren, B. Sugden, *Nature* **313**, 812 (1985).
6. D. R. Rawlins, G. Milman, S. D. Hayward, G. S. Hayward, *Cell* **42**, 859 (1985).
7. S.-H. Kung and P. G. Medveczky, *J. Virol.* **70**, 1738 (1996).
8. J. J. Russo *et al.*, *Proc. Natl. Acad. Sci. U.S.A.* **93**, 14862 (1996).
9. P. Kellam *et al.*, *J. Hum. Virol.* **1**, 19 (1997); L. Rainbow *et al.*, *J. Virol.* **71**, 5915 (1997); D. H. Kedes, M. Lagunoff, R. Renne, D. Ganem, *J. Clin. Invest.* **100**, 2606 (1997); F. Neipel, J. C. Albrecht, B. Fleckenstein, *J. Virol.* **71**, 4187 (1997).
10. J. C. Albrecht *et al.*, *J. Virol.* **66**, 5047 (1992); H. W. Virgin IV *et al.*, *ibid.* **71**, 5894 (1997).
11. S. J. Gao *et al.*, *Nature Med.* **2**, 925 (1996); D. H. Kedes *et al.*, *ibid.*, p. 918; D. Jones *et al.*, *N. Engl. J. Med.* **339**, 444 (1998); R. Renne *et al.*, *Nature Med.* **2**, 342 (1996).
12. L. Szekely *et al.*, *J. Gen. Virol.* **79**, 1445 (1998).
13. FISH was performed with TSA-Direct (NEN Life Science Products). Colcemid treatment and hypotonic swelling of cells was performed as described in (19). Cells were fixed in 4% paraformaldehyde at room temperature for 10 min and then fixed in 70% ethanol at 4°C for 10 min. Fixed cells were permeabilized with 0.5% Triton-X 100 and overlaid with DNA in situ hybridization solution (DAKO, Carpinteria, CA) containing 20 ng of a probe that was labeled with biotin and nick translated from pBSLANA. pBSLANA was constructed by subcloning the 4.7-kb KSHV genomic Sac I fragment flanking ORF 73 from the L54 library phage (8) into pBluescript (Stratagene). After denaturation of DNA at 93°C for 5 min, slides were incubated for 4 hours at 37°C, washed in 0.2× standard saline citrate for 30 min at 45°C, and blocked in TNB (0.1 M tris-HCl, pH 7.5, 0.15 M NaCl, 0.5% blocking reagent) at room temperature for 30 min. Slides were then incubated with streptavidin-horseradish peroxidase (1:100) for 30 min at 37°C and incubated with cyanine 3-tyramide (1:50) for 10 min at room temperature. After FISH, cells were incubated with BJAB cell extract-adsorbed KSHV immune serum (1:50) followed by secondary fluorescein isothiocyanate-conjugated antibody and counterstained with DAPI (1 µg/ml) in methanol for 15 min. For two-color fluorescence, DAPI was omitted.
14. Genomic ORF 73 was cloned downstream of the simian virus 40 (SV40) promoter in pSG5 (Stratagene) (termed pSG5LANA) or in pSG5FLAG [E. Hatzivassiliou, P. Cardot, V. I. Zannis, S. A. Mitsialis, *Biochemistry* **36**, 9221 (1997)] (termed pSG5 F-LANA). In pSG5 F-LANA, the four NH₂-terminal LANA amino acids are replaced with the FLAG epitope (DYKDDDDKV) (22). LANA stable cell lines were generated by electroporating pSG5LANA or pSG5 F-LANA and a plasmid encoding the hygromycin-resistance gene downstream of an SV40 promoter into BJAB cells [K. M. Kaye, K. M. Izumi, G. Mosialos, E. Kieff, *J. Virol.* **69**, 675 (1995); D. Liebowitz, J. Mannick, K. Takada, E. Kieff, *ibid.* **66**, 4612 (1992)]. After 48 hours, cells were seeded into microtiter plates, and hygromycin-resistant clones were selected. Hygromycin-resistant BJAB cells expressing pSG5LANA or pSG5

- F-LANA were transfected with 25 µg of the Z6 or Z8 cosmid. Z6 contains KSHV sequence including the terminal repeats and the first ~33 kb of the BC-1 genome cloned into S-Cos1 (Stratagene), and Z8 contains nucleotides ~73,000 to 107,000 of BC-1 KSHV cloned into S-Cos1 (8). S-Cos1 encodes the neomycin-resistance gene downstream of an SV40 promoter and provides G418 resistance. After 48 hours, cells were plated under G418 selection. For subclone analysis, the Z6 cosmid was digested with Hind III and religated, resulting in the deletion of KSHV sequences after the first ~13 kb of the genome (Z6-13). The two largest remaining Z6 KSHV Hind III fragments of ~7 and ~11 kb were cloned into pREP9 (Invitrogen) after the deletion of the pREP9 sequences between Cla I and Kpn I (Z6-7 and Z6-11 respectively). pREP9 encodes the neomycin-resistance gene downstream of a thymidine kinase promoter and provides G418 resistance. The Z6 subclones were transfected into BJAB/F-LANA or BJAB cells and selected for G418 resistance as above.
15. M. E. Ballestas and K. M. Kaye, unpublished data.
16. Gardella gels were prepared as previously described

- [T. Gardella, P. Medveczky, T. Sairenji, C. Mulder, *J. Virol.* **50**, 248 (1984)].
17. A. Bochkarev *et al.*, *Cell* **84**, 791 (1996).
18. D. Reisman and B. Sugden, *Mol. Cell. Biol.* **6**, 3838 (1986).
19. L. Petti, C. Sample, E. Kieff, *Virology* **176**, 563 (1990).
20. E. Grogan *et al.*, *Proc. Natl. Acad. Sci. U.S.A.* **80**, 7650 (1983); B. M. Reedman and G. Klein, *Int. J. Cancer* **11**, 499 (1973).
21. C. W. Lehman and M. R. Botchan, *Proc. Natl. Acad. Sci. U.S.A.* **95**, 4338 (1998); M. H. Skiadopoulos and A. A. McBride, *J. Virol.* **72**, 2079 (1998); A. Harris, B. D. Young, B. E. Griffin, *ibid.* **56**, 328 (1985).
22. Single-letter abbreviations for the amino acid residues are as follows: D, Asp; K, Lys; V, Val; and Y, Tyr.
23. R. Renne, M. Lagunoff, W. Zhong, D. Ganem, *J. Virol.* **70**, 8151 (1996).
24. We thank E. Kieff for helpful discussions and P. Marks for assistance with microscopy for Fig. 2. This work was supported by grant CA67380-04 (K.M.K.) from the National Cancer Institute.

3 November 1998; accepted 23 March 1999

A Role for DNA-PK in Retroviral DNA Integration

René Daniel, Richard A. Katz, Anna Marie Skalka*

Retroviral DNA integration is catalyzed by the viral protein integrase. Here, it is shown that DNA-dependent protein kinase (DNA-PK), a host cell protein, also participates in the reaction. DNA-PK-deficient murine *scid* cells infected with three different retroviruses showed a substantial reduction in retroviral DNA integration and died by apoptosis. *Scid* cell killing was not observed after infection with an integrase-defective virus, suggesting that abortive integration is the trigger for death in these DNA repair-deficient cells. These results suggest that the initial events in retroviral integration are detected as DNA damage by the host cell and that completion of the integration process requires the DNA-PK-mediated repair pathway.

Integration is an essential step in retroviral replication (1). Processing (nicking) of the viral DNA 3' ends and joining of these ends to staggered phosphates in the host DNA are carried out by the viral integrase (IN) protein (2). The initial linkage between viral and host DNA is a gapped intermediate in which the viral DNA 5' ends are unjoined. The processing and joining steps in the integration reaction have been reconstituted in vitro, with purified retroviral integrases and model viral and host DNA substrates. Repair of the gaps in vivo results in a 4- to 6-base pair repeat of host DNA flanking each proviral end, but this final step has not yet been reproduced in vitro. It has been reported that inhibition of a host DNA repair-related protein, poly(adenosine diphosphate-ribose) polymerase, blocks retroviral integration (3). Although it is generally assumed that host cell repair enzymes complete the integration reac-

tion, the pathways responsible and the mechanism by which repair is accomplished have not been identified.

In mammalian cells, repair of double-stranded DNA breaks by nonhomologous end joining (NHEJ) is mediated by DNA-dependent protein kinase (DNA-PK). DNA-PK is composed of a DNA-binding Ku70/Ku86 heterodimer and a large catalytic subunit, DNA-PK_{cs} (4). DNA-PK also functions in V(D)J recombination, and the underlying genetic defect in the V(D)J recombination-deficient, severe combined immunodeficiency (*scid*) mouse (5) is a truncation mutation of DNA-PK_{cs} (6). Thus, *scid* cell lines and primary cells are deficient in DNA-PK activity (7).

To investigate whether DNA-PK has a role in the repair process that completes retroviral integration, we infected *scid* cells with retrovirus vectors. *scid* pre-B cell lines S7, S29, and S33 and a control, normal cell line, N2 (8), were first infected with an avian retrovirus vector, encoding an amphotropic envelope protein that allows infection of a wide variety of mammalian cells [RCASBP-M(4070A), hereafter abbreviated R/M] (9). The results (Fig. 1A) were striking;

Institute for Cancer Research, Fox Chase Cancer Center, 7701 Burholme Avenue, Philadelphia, PA 19111, USA.

*To whom correspondence should be addressed. E-mail: AM_Skalka@fccc.edu